# Biochemical and biomechanical comparisions of decellularized scaffolds derived from porcine subcutaneous and visceral adipose tissue

**Maohui Lin[1]\*, Jinbo Ge[1]\*, Xuecen Wang[1]\*,
Ziqing Dong[1], Malcolm Xing[2,3], Feng Lu[1]
and Yunfan He[1]** (iD)

## Abstract

Decellularized adipose tissue (DAT) is a promising biomaterial for adipose tissue engineering. However, there is a lack of research of DAT prepared from xenogeneic porcine adipose tissue. This study aimed to compare the adipogenic ability of DAT derived from porcine subcutaneous (SDAT) and visceral adipose tissue (VDAT). The retention of key collagen in decellularized matrix was analysed to study the biochemical properties of SDAT and VDAT. For the biomechanical study, both DAT materials were fabricated into three-dimensional (3D) porous scaffolds for rheology and compressive tests. Human adipose-derived stem cells (ADSCs) were cultured on both scaffolds to further investigate the effect of matrix stiffness on cellular morphology and on adipogenic differentiation. ADSCs cultured on soft VDAT exhibited significantly reduced cellular area and upregulated adipogenic markers compared to those cultured on SDAT. In vivo results revealed higher adipose regeneration in the VDAT compared to the SDAT. This study further demonstrated that the relative expression of collagen IV and laminin was significantly higher in VDAT than in SDAT, while the collagen I expression and matrix stiffness of SDAT was significantly higher in comparison to VDAT. This result suggested that porcine adipose tissue could serve as a promising candidate for preparing DAT.

[1]Department of Plastic and Cosmetic Surgery, Nanfang Hospital, Southern Medical University, Guangzhou, P.R. China
[2]Departments of Mechanical Engineering, and Biochemistry and Medical Genetics, University of Manitoba, Winnipeg, MB, Canada
[3]Children's Hospital Research Institute of Manitoba, Winnipeg, MB, Canada

\*Maohui Lin, Jinbo Ge and Xuecen Wang contributed equally and are co–first authors.

**Corresponding authors:**
Yunfan He, Department of Plastic and Cosmetic Surgery, Nanfang Hospital, Southern Medical University, 1838 Guangzhou North Road, Guangzhou 510515, Guangdong, P.R. China.
Email: doctorheyunfan@hotmail.com

Feng Lu, Department of Plastic and Cosmetic Surgery, Nanfang Hospital, Southern Medical University, 1838 Guangzhou North Road, Guangzhou 510515, Guangdong, P.R. China.
Email: doctorlufeng@hotmail.com

Malcolm Xing, Departments of Mechanical Engineering, and Biochemistry and Medical Genetics, University of Manitoba, Winnipeg, MB R3T 2N2, Canada.
Email: malcolm.xing@umanitoba.ca

## Introduction

Reconstruction of subcutaneous soft-tissue defects presents a major challenge in plastic and reconstructive surgery. The current methods involve artificial material filling or autologous tissue transplantation. However, some disadvantages, including the occurrence of capsular contracture, resorption, necrosis and donor site morbidity, may limit the applications of these methods.[1–3] Therefore, there is a growing need for biomaterials that can not only replace lost or damaged soft tissue but also encourage its natural adipose regeneration. Decellularized extracellular matrix (ECM) derived from many living tissues have emerged as an ideal biomaterial for a broad range of regenerative medicine since the composition, architecture and physical properties of decellularized ECM provide specific physical and chemical cues for cell recruitment, proliferation and differentiation.[4] Clinical decellularized products are harvested from a variety of allogeneic or xenogeneic tissue sources, including dermis, urinary bladder, small intestine, mesothelium, pericardium and heart valves, and from several different species. Many decellularized products derived from allogeneic or xenogeneic tissue sources (e.g. dermis, urinary bladder and small intestine)[5–9] have been developed and used in the humans for wound repair and tissue regeneration. Adipose tissue represents a potentially abundant source of ECM and decellularization of adipose tissue was first described by Flynn[10] in 2010. Subsequently, several published articles have reported alternative methods for decellularizing adipose tissue[11,12] and decellularized adipose tissue (DAT) was found to provide an inductive microenvironment for adipogenesis both in vivo and in vitro.[13–17] In recent years, several groups have been testing DAT in vitro and in vivo for potential clinically translatable, tissue-engineering applications.[18–20] Most recently, Kokai et al.[21] reported a first allograft implantation of DAT in the dorsal wrist of patients. The DAT matrix maintained soft-tissue volume in the dorsal wrist in a 4-month investigation with no severe adverse events and adipogenesis was found in the matrix, indicating that DAT could serve as a biomaterial product for clinical soft-tissue filling in the future. Porcine adipose tissue is an abundant animal tissue.[22] More than 6.8 million tonnes of porcine adipose tissue are produced worldwide, with significant quantities of inedible adipose tissue being discarded.[15] Moreover, pigs have similar anatomical and physiological properties to humans,[23] so porcine adipose tissue may be an attractive candidate biomaterial for preparing DAT. Since pigs are abundant in both subcutaneous adipose tissue and visceral adipose tissue, which have significantly different appearance and texture, comparing DAT from two donor sites and determining an optimal porcine DAT preparation site are necessary.

While the mechanisms underlying ECM-mediated constructive remodelling are not completely understood, many studies have shown that different elements of the decellularized matrix impact regeneration.[24] The impact of biochemical properties of decellularized matrix on tissue regeneration has been a hot topic in the past decade.[25–27] For example, Reing et al.[28] and Agrawal et al.[29] reported that ECM degradation peptides possessed chemotactic and mitogenic activities for host progenitor cells. Huleihel et al.[30] and Dziki et al.[31] showed that matrix-bound nanovesicles promoted a transition in macrophage behaviour from a proinflammatory to a regulatory/anti-inflammatory phenotype, which in turn contribute to a constructive and functional tissue repair. Biochemical properties are also affecting tissue remodelling of decellularized matrix. Biomechanical study of DAT was first reported by Omidi and colleagues[32,33] who measured the mechanical properties of DAT samples derived from multiple fat depots and found that the mechanical properties of the DAT samples, including linear and hyperelastic properties, were similar to those of natural ex-vivo breast adipose tissue, suggesting the biomechanical suitability of DAT for breast reconstruction. Costa et al.[34] reported that decellularized urinary bladder matrix exhibited a rapid initial decrease in strength and modulus in Sprague Dawley rats of abdominal wall defect. This remodelling process was associated with a rapid, disproportionate loss of strength that was comparable or above that of the native abdominal wall. Edwards et al.[35] demonstrated that decellularization affects collagen crimp, tissue swelling and collagen fibre sliding of porcine superflexor tendon (pSFT), but the ample strength and integrity remains sufficient for the pSFT to act as a viable regenerative graft.

This study aimed to compare the adipogenic induction ability of both porcine subcutaneous DAT (SDAT) and visceral DAT (VDAT) and preliminarily investigate the effect of both biochemical and biomechanical factors on affecting the adipose regeneration of these two types of DATs.

## Materials and methods

### Preparation of porcine SDAT and VDAT

Porcine subcutaneous adipose tissue (abdominal subcutaneous adipose tissue) and visceral adipose tissue (omental adipose tissue) were obtained from a local slaughter house and transported on ice to the lab. Immediately after arrival, the tissues were cut into small pieces and washed thoroughly with distilled water.

The cut adipose tissue was decellularized following a protocol described by Flynn[10] after a slight modification. Briefly, the tissue was subjected to three cycles (1 h each) of freezing and thawing ($-80°C$ to $37°C$) in distilled water, followed by 0.05% trypsin digestion for 16 h at $37°C$ under constant agitation. After washing with phosphate-buffered solution (PBS), the samples underwent 48 h of polar solvent extraction in 99.9% isopropanol to remove the lipid content. Following three PBS washes, the samples were incubated for 16 h with Benzonase digestion solution (Sigma, St. Louis, USA), rinsed again three times with PBS and subjected to a final polar solvent extraction in 99.9% isopropanol for 8 h to remove the remaining lipid. At the end, the processed tissues were rinsed and disinfected with

0.1% peracetic acid in 4% ethanol for 4 h. The prepared SDAT and VDAT were stored in sterile PBS containing 1% penicillin–streptomycin at 4°C for short-term storage and the usage was carried out within 36 h.

## Evaluation of DAT

Both SDAT and VDAT samples were fixed in 4% paraformaldehyde and embedded in paraffin. Then 5-μm sections were cut for haematoxylin and eosin (HE). In addition, residual DNA was extracted using a DNeasy kit (Qiagen, Valencia, CA, USA). DNA content (μg/mg wet weight) was then quantified with a microplate reader (Model 680; Bio-Rad, Hercules, CA, USA) at 260 nm and normalised to the initial wet weight of each sample.

## Scanning electron microscopy

The inner structure of the two types of DAT was observed using scanning electron microscopy (SEM) (Hitachi S-3000N; Hitachi Ltd., Tokyo, Japan). The samples were fixed to metal stubs and coated with platinum by a sputter. An acceleration voltage of 20 kV was used, and images were observed using Canon digital camera (Canon Inc., Tokyo, Japan).

## Key protein evaluations of SDAT and VDAT

Both SDAT and VDAT samples were fixed in 4% paraformaldehyde and embedded in paraffin. Then 5-μm sections were cut for fluorescence staining of collagen I (ab21286, Abcam), collagen IV (ab19808, Abcam) and laminin (ab11575, Abcam) in a primary antibody overnight at 4°C. The primary antibodies were detected with the appropriate secondary antibodies, and sections were observed using a confocal laser-scanning microscope (FV10i-W; Olympus, Tokyo, Japan).

Biochemical assays were performed for the quantification of collagen I (JYM0195Po, ELISA LAB, Wuhan, China), collagen IV (JYM0245Po, ELISA LAB, Wuhan, China) and laminin (JYM0040Po, ELISA Lab, Wuhan, China) in SDAT and VDAT by sensitivity enzyme-linked immunosorbent assay (ELISA) kits. Dry DAT specimens and native adipose tissue specimens with same dimension were thoroughly sheared and homogenated via a homogeniser. The complex was precipitated by centrifugation at 3000 g for 20 min. The supernatant was collected and dissolved in 1 mL dissociation reagent. Protein concentrations were then measured according to the manufacturer's instructions.

## Preparation of DAT scaffolds and mechanical characterization measurement

To evaluate biomechanical properties, both SDAT and VDAT were fabricated into three-dimensional porous scaffolds as previously described.[36] Briefly, equal amounts of SDAT and VDAT were suspended with equal amounts of distilled water, respectively, gently poured into cylindrical moulds, frozen at −80°C and lyophilised in a freeze dryer.

The DAT specimens (1.5 cm height, 1.3 cm diameter) were prepared in moulds according to the above protocol and kept hydrated with $1 \times PBS$. Rheology measurements of DAT scaffolds and native adipose tissue with same dimension were performed using a TA Discovery Hybrid Rheometer at 25°C, with a steel parallel plate of 8-mm-diameter geometry. The strain was set up as 0.5%, and the frequency increased from 0.1 to $100 \, rad \, s^{-1}$ by steps. Compression tests were performed up to 80% compressive strain at a speed of 20 mm/min. The compression tests were executed on a universal tensile tester (Instron 5965), equipped with a pair of compression plates and a 500 N loading cell.

## Animal study

Four- to six-week-old female C57BL/6 mice were purchased from the Southern Medical University Laboratory Animal Centre and maintained in microisolator cages at the Animal Experiment Centre of Nanfang Hospital. All animal procedures were approved by the Nanfang Hospital Institutional Animal Care and Use Committee, in accordance with the guidelines of the National Health and Medical Research Council of China. Two types of DAT scaffolds were transplanted subcutaneously into either side of the back of each mouse. Mice were sacrificed at week 6 and week 12 (n = 6 for each time point in each group), and the grafts were explanted. Each sample was divided into two parts. One half of the samples were fixed in 4% paraformaldehyde, embedded in paraffin. The remainder samples were frozen and preserved at −80°C for RNA analysis.

## Masson staining and immunostaining of harvested samples

Samples were sectioned into 5-μm thickness slices and stained with Masson's trichrome for collagen analysis. Immunostaining was performed to analyse angiogenesis and adipogenesis in samples. Immunostaining of angiogenesis and adipogenesis markers were performed with antibody against CD31 (ab28364; Abcam, Cambridge, UK). The incubation of primary antibodies lasted for 15 h at 4°C followed by incubation of appropriate secondary antibodies. The sections were counterstained with Hematoxylin in CD31 sections or DAPI (4′,6-diamidino-2-phenylindole) in perilipin sections. Angiogenesis in implants was assessed by counting the number of CD31-positive vessels by the total number of cells shown from four fields of each slide. The cell counting was performed by two blinded evaluators. Adipocytes and nuclei were identified by perilipin and
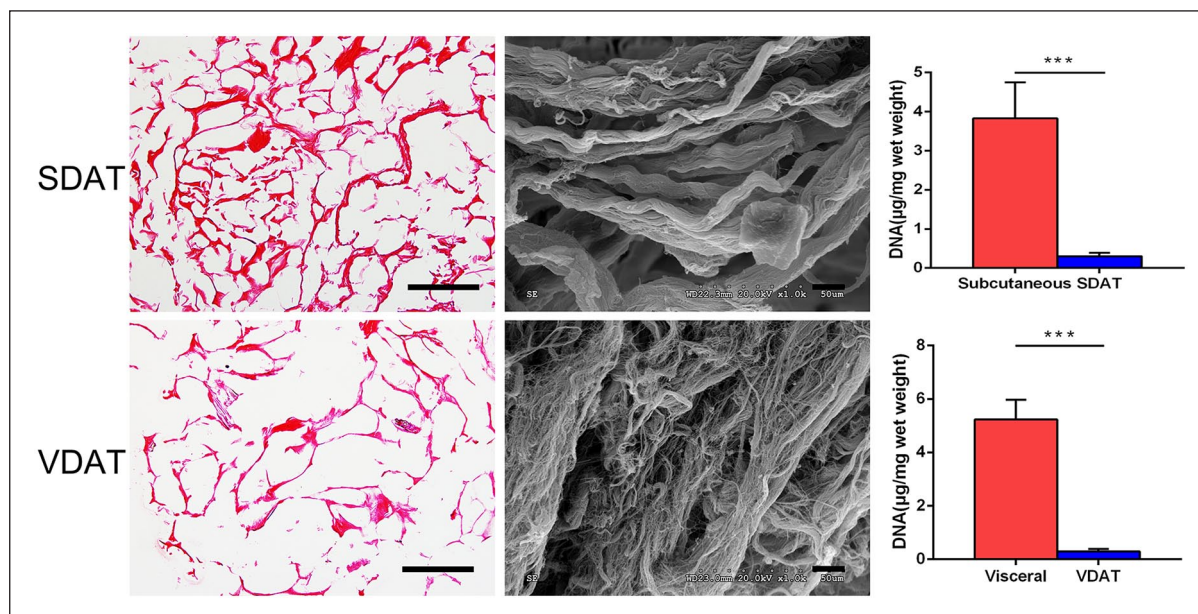
**Figure 1.** DAT characterization.
HE staining (scale bars = 200 μm), SEM analysis (scale bars = 10 μm) and residual DNA quantification of SDAT and VDAT.
***p < 0.001.

DAPI staining, respectively. The adipogenesis area was calculated as follows: Adipocytes Area Rate (100%) = Adipocytes area/Total area × 100%. The calculation was performed by two blinded evaluators.

### Cell culture and staining

Passage 3 adipose-derived stem cells (ADSCs) were obtained from the Research Center of Clinical Medicine of Nanfang Hospital and used in the following experiment.

Disc-shaped DAT scaffolds (diameter, 1 cm; height, 0.5 cm) were prepared according to the above protocol and placed in 24-well plates. A suspension of human ADSCs containing $5 \times 10^4$ cells was seeded onto the two types of DAT scaffolds and allowed to attach overnight.

To evaluate the effect of two DAT scaffolds on the adipogenesis of ADSCs, the wells of SDAT and VDAT were treated with 2-mL fresh media or 2-mL adipogenic media (DMEM/F12 plus 10% FBS, 500 mM isobutylmethylxanthine, 1 mM dexamethasone, 10 mg/mL insulin, 200 mM indomethacin, 100 IU penicillin and 100 mg/mL streptomycin), respectively. Each respective medium was then changed every 3 days until completion of the study.

To evaluate the effect of two DAT scaffolds on the cytoskeletal organisation, scaffold-seeded ADSCs were rinsed twice and fixed in 4% paraformaldehyde at day 3 and day 14. Cytoskeletal organisation (F-actin distribution) within the cells was identified using phalloidin (P1951, Sigma) staining. Cells were incubated in staining buffer (1% bovine serum albumin and 0.3% Triton X-100 in PBS) for 30 min to block nonspecific binding. Phalloidin

was diluted 1:40 in staining buffer and added to the cells for 20 min. Nuclei were counterstained with DAPI. After rinsing, the cells were imaged using a confocal laser-scanning microscope.

### Quantitative reverse-transcription polymerase chain reaction

Total RNA was extracted from samples using TRIzol Reagent (Invitrogen/Life Technologies, Carlsbad, CA, USA) following the manufacturer's protocol. Extracted RNA was quantified using a Thermo Scientific NanoDrop 2000c. Superscript III reverse transcriptase (Life Technologies) was used to convert the RNA template into cDNA, following the manufacturer's protocol. Quantitative reverse-transcription polymerase chain reaction (qRT-PCR) was conducted on a StepOnePlus Real-Time PCR System using SYBR Green Master Mix (Life Technologies). PCR specificity was assessed using the cycle threshold method. Relative expression of target genes was normalised to that of glyceraldehyde 3-phosphate dehydrogenase (GAPDH), the endogenous control gene.

### Statistical analysis

Quantitative results were presented as the mean ± standard deviation. Statistical analysis was performed using SPSS 21.0 software (IBM Corp., Armonk, NY, USA). Student's *t*-test was used to compare two groups at a single time point and a one-way analysis of variance was employed to compare groups at all time points. A value of p < 0.05 was considered significant.

## Result

### DAT characterization

H & E staining revealed that no obvious nuclei were evident in both SDAT and VDAT. SEM analysis showed that these two DAT were mainly composed of collagen fibres of different diameters, and no lipid droplets could be detected inside the tissue. Moreover, multiple thick collagen fibre could be found in SDAT scaffolds, and the average fibre diameter of SDAT is significantly larger than that of VDAT. Compared to the subcutaneous porcine adipose tissue
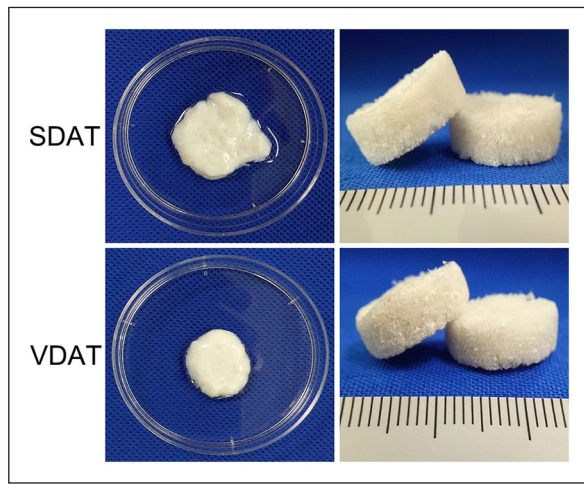


**Figure 2.** DAT scaffolds characterization.
Macroscopic view of SDAT and VDAT scaffolds.

$(3.8 \pm 0.9\,\mu g/mg)$ and visceral adipose tissue $(5.2 \pm 0.7\,\mu g/mg)$, the DNA content of the SDAT $(0.3 \pm 0.08\,\mu g/mg)$ and VDAT $(0.3 \pm 0.1\,\mu g/mg)$ was significantly reduced $(***p < 0.001)$, indicating the effective removal of cellular components (Figure 1).

SDAT and VDAT were fabricated into three-dimensional (3D) scaffolds with round dish shape (Figure 2). The 3D scaffolds had a highly porous structure and exhibit an elastic behaviour.

### Collagen staining and volume retention of two DAT scaffolds in vivo

A large quantity of collagen area (blue) was observed in both SDAT and VDAT scaffolds at week 6 and cell infiltration were observed in collagen during the same period. At week 12, collagen adipose tissue development observed in the collagen infiltrated cells were mainly concentrated around these newly developed adipocytes (Figure 3(a)). The volume of DAT scaffolds decreased from week 0 to week 6 and the remained volume of SDAT was significantly less than that of VDAT at week 12 (p < 0.05) (Figure 3(b)).

### Angiogenesis and adipogenesis in vivo

Angiogenesis in implants was assessed by CD31 staining. Numerous neo-vessels were observed in both implants at week 6, and the number of neo-vessels decreased at week 12 (Figure 4(a)). Quantification analysis revealed that the
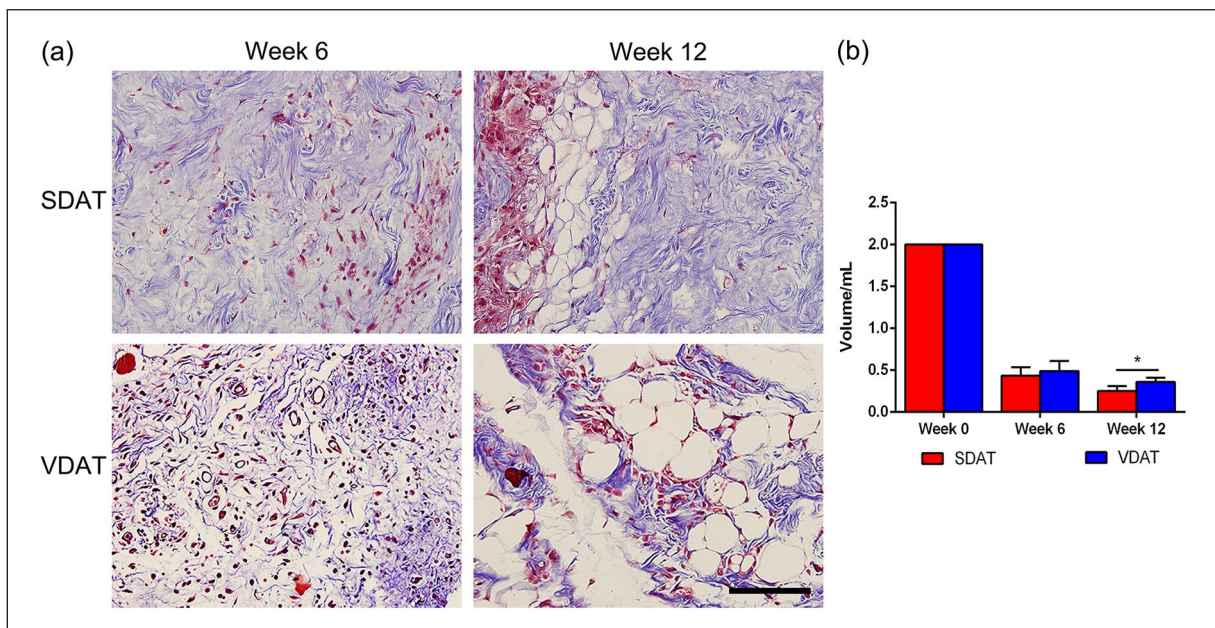


**Figure 3.** Collagen staining and volume retention of two DAT scaffolds: (a) Images of two DAT scaffolds from in vivo study after collagen staining and (b) volume retention of two DAT scaffolds.
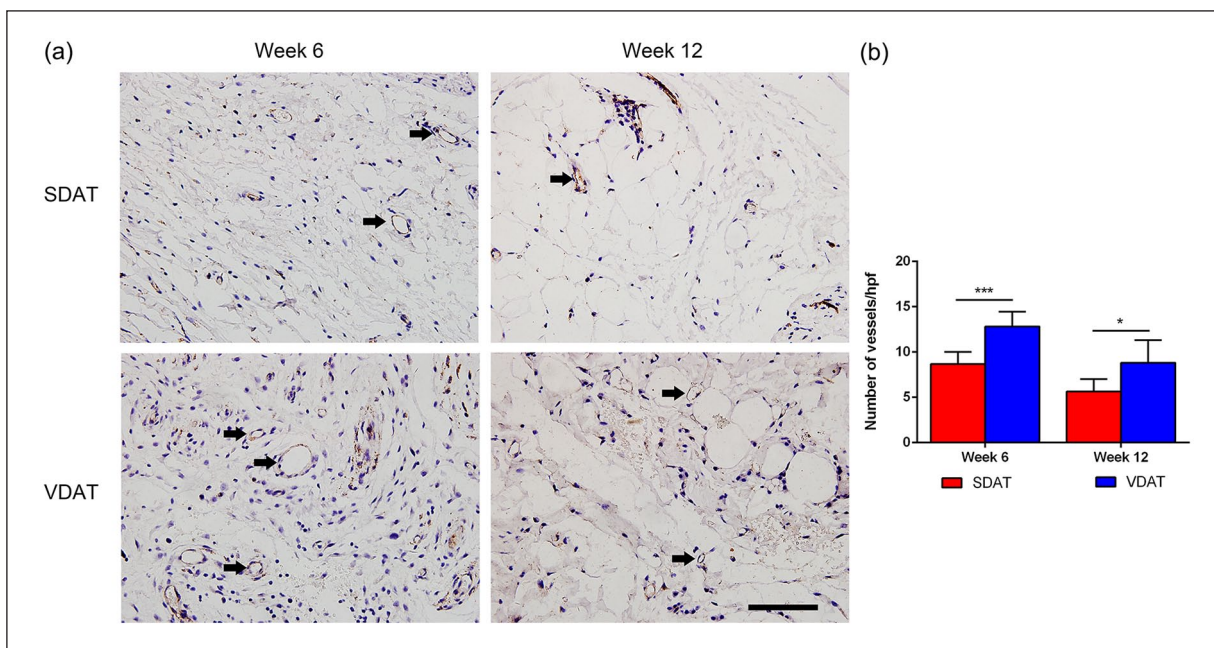Scale bars = 400 μm.
*p < 0.05.

**Figure 4.** In vivo angiogenesis of DAT scaffolds: (a) CD31 staining of neo-vessels and (b) quantification of neo-vessels in both DAT implants.
Scale bars = 400 μm.
*p < 0.05. ***p < 0.001.

number of neo-vessels in VDAT implants was significantly higher than that in SDAT implants from week 6 to week 12 (Figure 4(b)).

In vivo adipogenesis of SDAT and VDAT was assessed by Perilipin staining. Adipocytes were observed within the peripheral region of the scaffolds at week 6 in two groups. At week 12, numerous mature adipocytes could be observed in the peripheral region of both SDAT and VDAT scaffolds (Figure 5(a)). Semi-quantification of adipose regeneration revealed an increased adipose regeneration area in both SDAT and VDAT plants from week 6 to week 12. The statistical analysis further revealed that the adipose regeneration area of VDAT was significantly higher than that of SDAT during the same period (p < 0.05) (Figure 5(b)). In addition, gene analysis demonstrated significantly higher expression of the adipogenic factor PPARγ in VDAT group than in the SDAT group at week 6 (p < 0.05) (Figure 5(c)).

### Retention of key ECM proteins

The relative retention of adipose key ECM proteins after decellularization in SDAT and VDAT was evaluated. Collagen I, collagen IV and laminin distribution was observed by fluorescence staining (Figure 6). Quantitative results revealed that the retention of collagen I and laminin was significantly reduced in SDAT and VDAT compared to native tissue, but the collagen IV is well preserved in decellularized tissue (Figure 7(a)). The content of collagen IV and laminin in VDAT is significantly higher than that in

SDAT (p < 0.001), while the expression of collagen I in SDAT is significantly higher than that in VDAT (p < 0.001) (Figure 7(b)).

### Mechanical properties of DAT scaffolds and native adipose tissue

When rheological properties of SDAT and VDAT scaffolds were measured under oscillation condition after total hydration, subcutaneous native adipose tissue (SNAT) and visceral native adipose tissue (VNAT) with same dimension were tested under identical condition, the assessment and comparison between different samples were performed with the storage modulus at angular frequency at 1 Hz which represented similar physiological stress between fat tissue and surrounding tissue.[37] All samples exhibited greater storage modulus than loss modulus which indicated the gel-like behaviour; the fat tissue after decellularization presented around one order higher than that of the native fat tissue from original sites which are according with the previous report,[38] for example, the storage modulus of VDAT and VNAT were $2.7 \times 10^5$ Pa and $2.5 \times 10^2$ Pa, respectively (Figure 8(a)).

The compressive tests of two DAT scaffolds were carried out in the present study in hydrated conditions analogous to the in vivo environment at room temperature. A typical elastic response of soft tissue could be observed in the compressive strain–stress curve, starting with a linear elastic response, followed by a transition region and
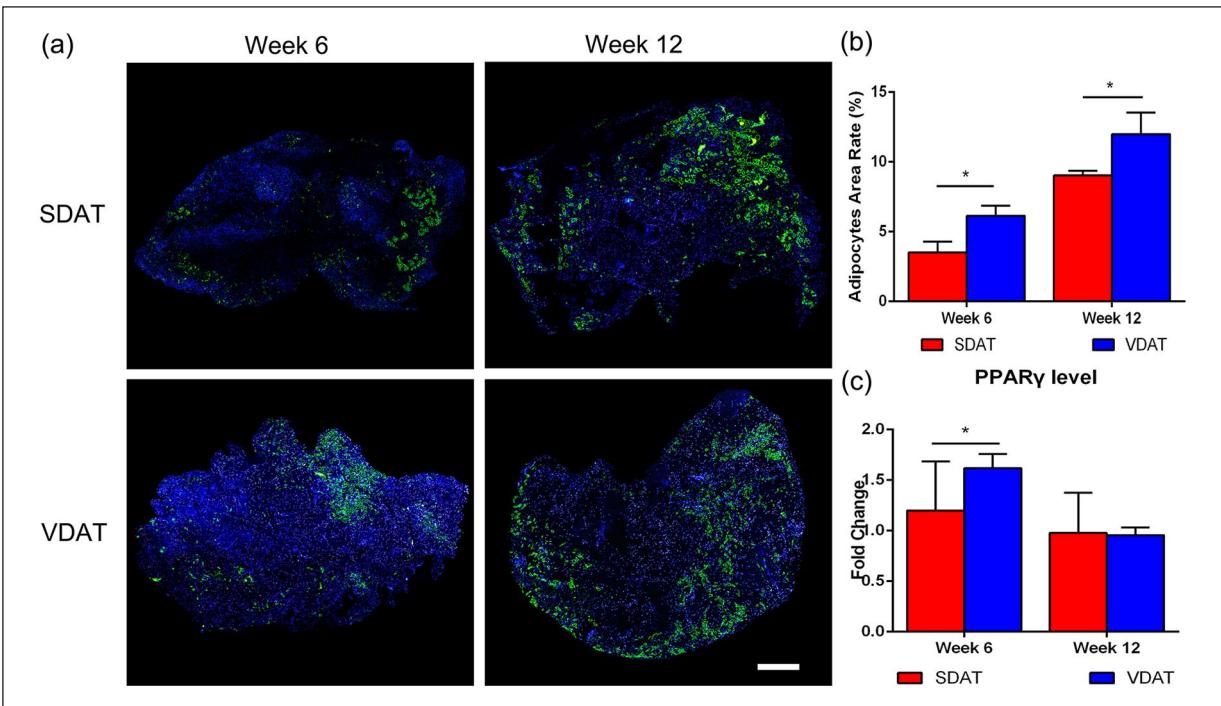
**Figure 5.** In vivo adipogenesis of DAT scaffolds: (a) Perilipin staining confirmed the adipogenesis in both groups at different time points, (b) quantification of adipocytes area rate in adipose constructs in both groups and (c) qRT-PCR analysis of PPARγ expression in both groups.
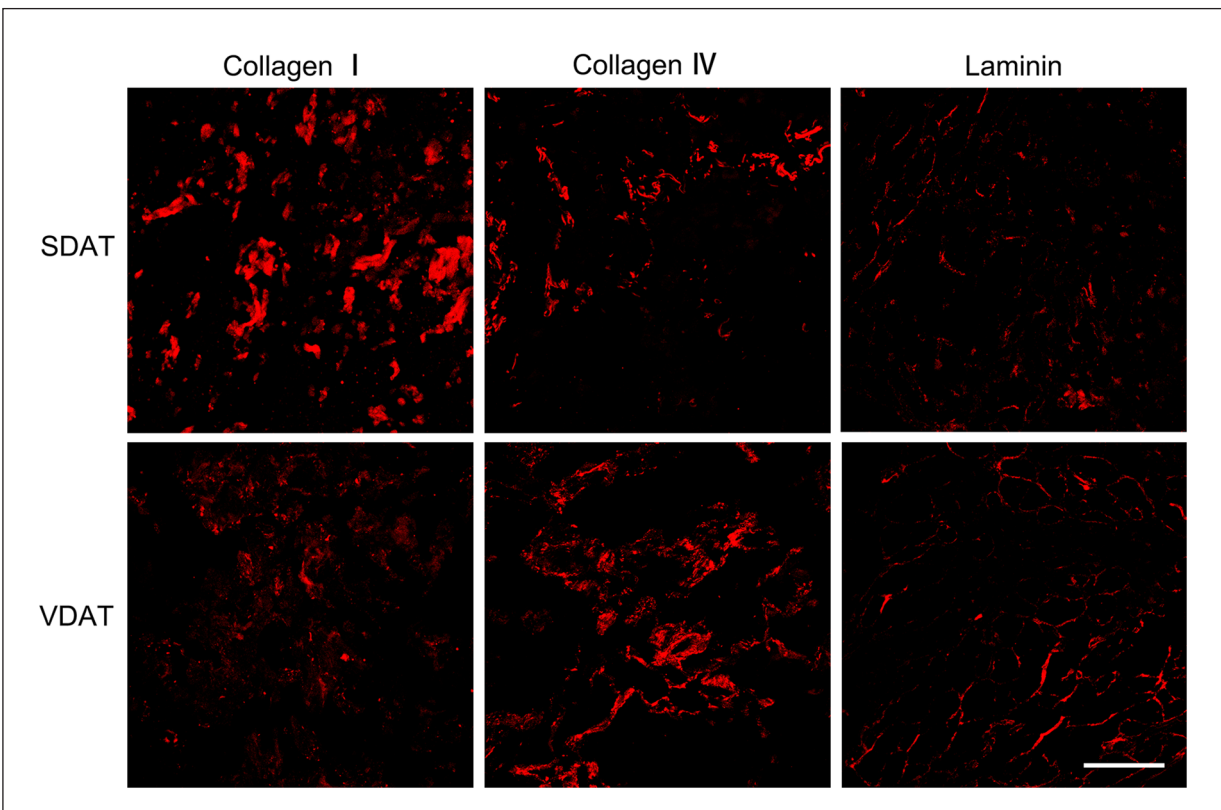Scale bars = 1000 μm.
*p < 0.05.



**Figure 6.** Fluorescence staining of collagen I, collagen IV and laminin in both types of DAT.
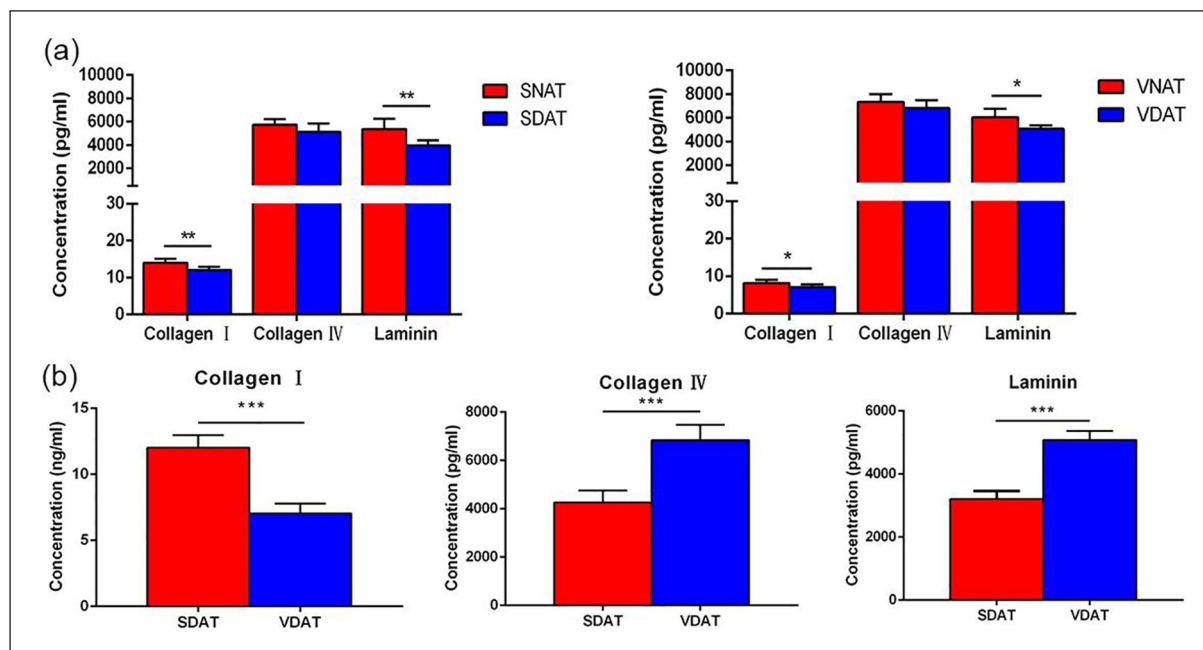Scale bars = 200 μm.

**Figure 7.** (a) The quantification of collagen I, collagen IV and laminin in decellularized adipose tissue and native adipose tissue and (b) comparison of collagen I, collagen IV and laminin expression in SDAT and VDAT.
$*p < 0.05$. $**p < 0.01$. $***p < 0.001$.

ending with a linear slope, which was referred as 'collagen dominant phase'; however, some remarkable differences were observed in the groups with different tissue sources. The Young's modulus of both groups was calculated at the initial linear portion. The value of VDAT scaffolds was $3.9 \pm 0.9$ kPa and the decellularized scaffolds (SDAT) from subcutaneous fat displayed a significant higher modulus than visceral source fat ($6.6 \pm 1.8$ kPa). The maximum stress that the scaffold could withstand before failure was called ultimate tensile strength (UTS). The UTS of SDAT ($0.2 \pm 15.3$ MPa) exhibited a significantly higher value than that of VDAT ($0.1 \pm 16.6$ MPa) (Figure 8(b)).

### Matrix stiffness modulates ADSCs morphology and differentiation

ADSCs were seeded on two DAT scaffolds in adipogenic media to investigate the adipogenic effect of DAT stiffness on ADSCs in vitro, and morphological changes associated with adipogenesis were quantified. By day 3, the cells on both DAT scaffolds exhibited characteristically elongated shape. By day 14, ADSCs on both scaffolds adopted a reduced cellular area and ADSCs on the soft VDAT scaffolds maintained a relatively compact, rounded shape compared to that on SDAT scaffolds (Figure 9(a)). The ADSCs on the VDAT scaffolds had a significantly smaller cell area than that on SDAT scaffolds at day 14 (Figure 9(b)). Quantitative RT-PCR analysis of adipogenic gene revealed that ADSCs on VDAT exhibited a

significant upregulation of PPARγ compared to ADSCs cultured on SDAT scaffolds at day 14 (Figure 9(c)).

## Discussion

Our studies showed that decellularized scaffolds can be prepared from both porcine subcutaneous and visceral adipose tissue and implanted subcutaneously for engineered adipose tissue construction. Both decellularized scaffolds supported cell migration and infiltration, and the infiltrated host cells mainly appeared at the periphery of the scaffolds. Masson staining revealed that both DAT scaffolds exhibited a characteristic of collagen remodelling; the adipose tissue development could be observed near the remodelling collagen, indicating that both DAT scaffolds have a characteristic of bioactive properties for adipose regeneration.

Biochemical studies performed in the present study indicated that both types of DAT retained key ECM collagen components (collagen I, collagen IV and laminin). Collagen serves as a primary structural element of the ECM. For example, Fibril-forming collagens (types I, II, III, V and XI) have a clear structural role of mechanical support and dimensional stability.[39] Moreover, specific components (e.g. basement membrane component, fibronectin and laminin) from the ECM have been extensively used as a biomaterial in cell culture or tissue repair for many years and have been shown to have profound effects on cells, both with respect to attachment and survival as well as for the maintenance of cellular functions.[40–42] In general, extracellular fibronectin and
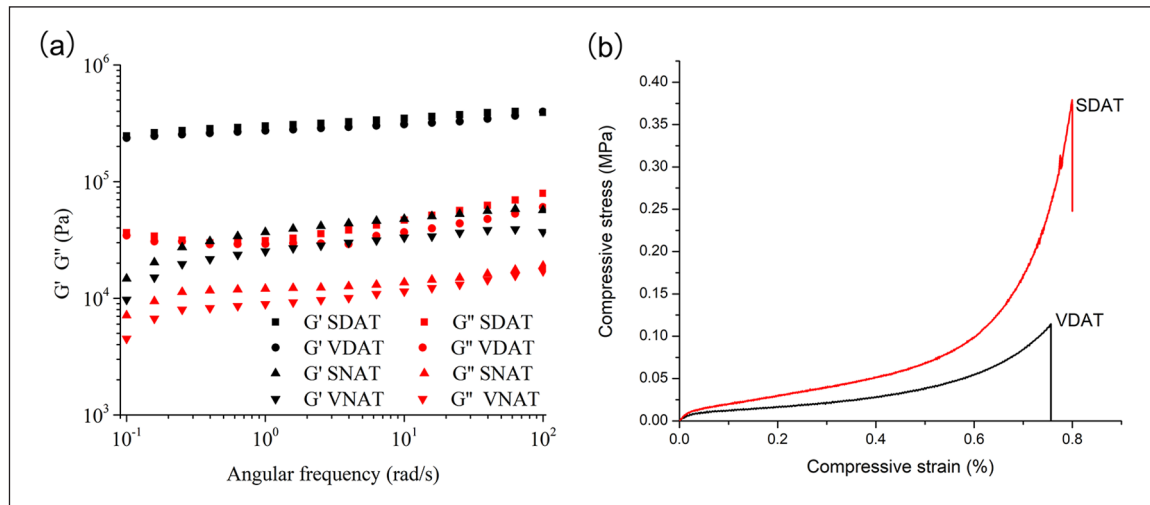
**Figure 8.** Biomechanical evaluation of DAT scaffolds and native adipose tissue: (a) Rheology measurement and (b) compression measurement.
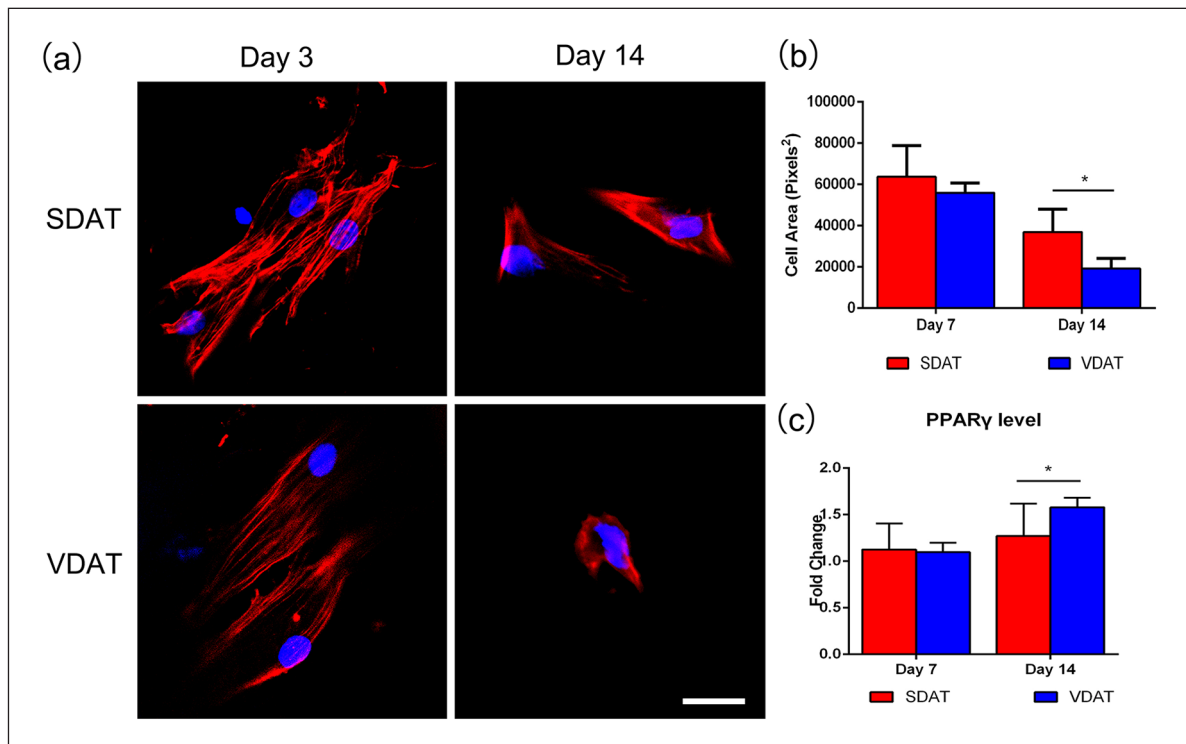


**Figure 9.** Effect of scaffolds stiffness on cell morphology: (a) Phalloidin staining of Cytoskeleton (F-actin), (b) cell area measurement and (c) adipogenic gene PPARγ expression.
Scale bars = 400 μm.
*p < 0.05.

laminin form networks with collagen fibres[13] and provide attachment points for integrins anchored in the adipocyte membrane.[43] Collagen VI is abundant in adipose tissue and attachment to Collagen VI is sufficient to restore adipogenic potential in preadipocytes with blocked collagen synthesis.[44] Collagen IV is present within the basement membrane that

enwraps each adipocyte and is important for angiogenesis[45,46]; laminin is distributed primarily around well-developed fat vacuoles, and it is upregulated during the adipogenesis of preadipocytes and lipogenesis of adipocytes.[47,48] Moreover, laminins are key glycoprotein components of basement membranes that present in all blood

vessels.[49] The interaction of endothelial cells with basement membrane components plays an essential role during angiogenic processes,[50] and proteolytic cleavage of laminins may affect their role in angiogenesis. Type I collagen molecules, staggered and interwoven with each other to form thick collagen bundles, provide the major ECM framework necessary to sustain the structure and function of tissues (e.g. skin, blood vessels, bone, tendon).[51] Biochemical analyses in this study revealed that the relative expression of collagen IV and laminin in VDAT is significantly higher than that in SDAT, which may partly explain the improved angiogenesis and adipose regeneration result in the VDAT implants, as compared with that in the SDAT implants.

The mechanical properties of the ECM are also considered to affect the progression of various cellular functions, such as proliferation, differentiation and ECM secretion.[52,53] In particular, the substrate biomechanics[54] as well as the topography of the environment[55] may modulate stem cell fate and 3D organisation in a way similar to biochemical signals. It has been shown that substrates elasticity may direct stem cell lineage specification through affecting the cellular focal-adhesion structure and the cytoskeleton.[56] Surface nanotopography of extracellular microenvironment could induce pronounced changes to cell shape and consequently gene expression, and this change could influence cellular responses from attachment and migration to differentiation and production of new tissues such as neuron and muscle.[55,57–59] Cells are highly sensitive to mechanical stimuli (e.g. compressive, tensile and shear) and the mechanical properties of their matrix.[60] On soft matrices, cells spread less and develop larger actin stress fibres than on soft matrices.[61] Histologic examinations revealed that the main protein components were preserved in both DAT matrix. Key ECM proteins (collagen I, collagen IV and laminin) in native adipose tissue (SNAT, VNAT) were measured and the comparison between native adipose tissue and DAT was made. The results revealed that the retention of collagen I and laminin was significantly reduced in SDAT and VDAT compared to native tissue, but the collagen IV is well preserved in decellularized tissue (Figure 7(a)). The reduction in collagen I and laminin in decellularized tissue compared to native tissue may be ascribed to the damage caused by chemical agents during decellularized process,[20,62] emphasising the importance of an optimal decellularization strategy that could achieve a good balance between optimal decellularization and maintaining matrix physical properties.[63,64] Further analysis demonstrated a significant higher relative expression of collagen I in SDAT than in VDAT and a weak mechanical strength of VDAT compared with SDAT. Moreover, collagen fibre network appeared looser and less crimped in VDAT. We further elucidated how substrate stiffness regulated adipose regeneration by culturing ADSCs on two DAT scaffolds. By quantifying the morphological changes associated with their differentiation, we found that consequence of culturing ADSCs on softer

substrates (VDAT) exhibited a compact, rounded shape, while cells on SDAT exhibited a more spreading morphology. Studies revealed that matrix stiffness also controls cell fate by directing the gene expression and the differentiation of mesenchymal stem cells.[56] In particular, matrices may direct differentiation towards lineages and the normal mechanical environment of which approximates that level of stiffness. A recent study by Young et al.[65] detailed a similar observation. Using decellularized human lipoaspirate to functionalise polyacrylamide gels of varying stiffness, they found that ADSCs on gels that mimicked the native matrix stiffness of adipose tissue (2 kPa) exhibited a significantly reduced cell area and upregulated adipogenic markers, indicating that biomechanical cues are capable of regulating adipogenesis. In this study, the smaller cellular area and the higher adipogenic gene PPARγ expression of ADSCs on VDAT compared to that on SDAT imply that the mechanical property of scaffolds may serve as another important factor that affects the adipose regeneration results between SDAT and VDAT.

There is a growing need for biomaterials that can not only replace lost or damaged adipose tissue but also facilitate its natural regeneration and continual integration with surrounding tissue throughout the lifetime of the patient. Although hyaluronic acid and collagen-based gels are available soft-tissue filler for filling subcutaneous voids in clinics, these materials fail to stimulate adipose regeneration and often suffer from limited longevity due to rapid resorption in vivo.[66,67] Our results suggested that future soft-tissue filler materials could incorporate DAT elements in order to restore the adipose deficits instead of simply filling them with static materials. Since the present study demonstrated that SDAT and VDAT have different mechanical stiffness, they could serve as available substitutes for filling soft-tissue defects that require various stiffness. As shown in Figure 2, both SDAT and VDAT can be fabricated into specific 3D shape in moulds through a lyophilization process. The 3D DAT scaffolds had a highly porous structure and exhibit highly elastic behaviour, even when wet. In previous studies, DAT displayed a highly customizable property and was often made into various formats, such as injectable gels,[13,21] powers,[12,36] microcarriers,[68] porous foams,[15] printing bioink[69] and so on. In addition, DAT was often used as one component composited with other materials, such as thermosensitive hydrogel composed of soluble methylcellulose and soluble DAT,[70] methacrylated glycol chitosan (MGC)–based or methacrylated chondroitin sulphate (MCS)–based composite scaffolds[71] and the DAT-fibroin hydrogels.[72] Therefore, it is reasonable to speculate that porcine adipose tissue can serve as xenogeneic biomaterials to produce anatomically relevant 3D DAT scaffolds that can address the need for on-demand tissue production. The customizable property of porcine DAT makes it a promising biomaterial to reconstruct soft-tissue defects (caused by complex traumas, oncologic resections, congenital abnormalities, etc.) of

various shape in clinics in a patient-specific manner. Autologous tissue transplantation is a still commonly used procedure to reconstruct soft-tissue defects in clinics.[37,73,74] However, this strategy is generally limited by certain limitations such as donor site morbidity and flap necrosis due to insufficient blood supply.[75,76] Obviously, using DAT as 'off-the-shelf' products to reconstruct soft-tissue defects would largely avoid the limitations caused by autologous tissue transplantation.

Consistent with previous studies,[12,13,36,77] in vivo implantation of SDAT and VDAT scaffolds without compositing cells or growth factors showed biocompatibility, and supported blood vessel and adipose regeneration in this study. However, a fast resorption of DAT scaffolds was observed after in vivo implantation. It is reported that collagen-based materials have seen rapid resorption and limited vascular formation following subcutaneous implantation.[78,79] DAT, on its own, did not encourage significant host adipogenesis.[80] However, DAT transplanted into the subcutaneous tissue as a scaffold composited with stem cells[68,81–83] or growth factors[84] could induce strong angiogenic response and preserve volume well. For example, rat ADSCs seeding significantly enhanced angiogenesis and adipogenesis of porcine DAT in rats.[83] Zhang et al.[85] described that DAT loaded with basic fibroblast growth factor exhibited a significantly increased implant retention compared to DAT alone in vivo over a period of 12 weeks. Similar results have been seen with collagen-based materials. Injections of fibrin gel alone were resorbed within 4 weeks in vivo but were able to maintain 50% of their original volume when adipocyte-differentiated ADSCs were incorporated.[86,87] Therefore, for long-term and stable volume retention of DAT in vivo, an incorporation of stem cells or growth factors is recommended. The DNA levels of porcine SNAT ($3800 \pm 900$ ng/mg) and VNAT ($5200 \pm 700$ ng/mg) detected in our study is higher than in porcine native adipose tissue ($1173 \pm 175$ ng/mg) described by Choi et al.[36] We speculated that this DNA difference may be ascribed to the breeds differences of pigs used in these two studies. Different mass of DNA detected in DAT was shown in articles. From low to high order, there have been $2.1 \pm 0.9$ ng/mg,[81] $6.57 \pm 3.49$ ng/mg,[88] $39 \pm 15$ ng/mg,[69] $43.52 \pm 6.17$ ng/mg,[89] $187 \pm 35$ ng/mg,[80] $230.7 \pm 44.5$ ng/mg[72] and around 600 ng/mg.[13] Compared to the porcine SNAT and visceral adipose tissue, the DNA levels of the SDAT ($300 \pm 80$ ng/mg) and VDAT ($300 \pm 100$ ng/mg) was significantly reduced (***$p < 0.001$). Although a DNA threshold of 50 ng/mg is considered as a safe amount for clinical applications,[62,90–92] there was no evidence that DNA > 50 ng/mg in the DAT would cause immune reaction or affect the growth and proliferation of cells. DAT is an ideal biomaterial for soft-tissue filling, but the underlying adipogenesis mechanisms of DAT still remain unclear. This preliminary study indicated that ECM composition and scaffold mechanical property are both likely to serve as important factors in affecting adipogenesis of DAT scaffolds. But the current study is small and data are limited,

further studies are still needed to fully explain the exact adipogenesis mechanisms between these two types of DAT scaffolds.

## Conclusion

Porcine adipose tissue can be fabricated into 3D scaffolds and VDAT scaffolds exhibit a better adipogenesis result compared with SDAT scaffolds in vivo. Both SDAT and VDAT scaffolds exhibited gel-like characteristic, with SDAT displayed a higher stiffness than VDAT. Collagen IV and laminin content is higher in VDAT compared to SDAT, while collagen I in SDAT is significantly higher than that in VDAT. Porcine adipose tissue could serve as a promising candidate for preparing DAT.

### ORCID iD

Yunfan He (iD) https://orcid.org/0000-0002-5681-4666

### References

1. Jurkiewicz MJ and Nahai F. The use of free revascularized grafts in the amelioration of hemifacial atrophy. *Plast Reconstr Surg* 1985; 76(1): 44–55.
2. Butterwick KJ, Nootheti PK, Hsu JW, et al. Autologous fat transfer: an in-depth look at varying concepts and techniques. *Facial Plast Surg Clin North Am* 2007; 15(1): 99–111, viii.
3. Luo L, He Y, Chang Q, et al. Polycaprolactone nanofibrous mesh reduces foreign body reaction and induces adipose flap expansion in tissue engineering chamber. *Int J Nanomedicine* 2016; 11: 6471–6483.
4. Kawecki M, Labus W, Klama-Baryla A, et al. A review of decellurization methods caused by an urgent need for quality control of cell-free extracellular matrix' scaffolds and their role in regenerative medicine. *J Biomed Mater Res B Appl Biomater* 2018; 106(2): 909–923.
5. Aamodt JM and Grainger DW. Extracellular matrix-based biomaterial scaffolds and the host response. *Biomaterials* 2016; 86: 68–82.

6. Chen RN, Ho HO, Tsai YT, et al. Process development of an acellular dermal matrix (ADM) for biomedical applications. *Biomaterials* 2004; 25(13): 2679–2686.

7. Skovsted Yde S, Brunbjerg ME and Damsgaard TE. Acellular dermal matrices in breast reconstructions – a literature review. *J Plast Surg Hand Surg* 2016; 50(4): 187–196.

8. Hughes OB, Rakosi A, Macquhae F, et al. A review of cellular and acellular matrix products: indications, techniques, and outcomes. *Plast Reconstr Surg* 2016; 138(3, Suppl.): 138S–147S.

9. Kneib C, von Glehn CQ, Costa FD, et al. Evaluation of humoral immune response to donor HLA after implantation of cellularized versus decellularized human heart valve allografts. *Tissue Antigens* 2012; 80(2): 165–174.

10. Flynn LE. The use of decellularized adipose tissue to provide an inductive microenvironment for the adipogenic differentiation of human adipose-derived stem cells. *Biomaterials* 2010; 31(17): 4715–4724.

11. Brown BN, Freund JM, Han L, et al. Comparison of three methods for the derivation of a biologic scaffold composed of adipose tissue extracellular matrix. *Tissue Eng Part C Methods* 2011; 17(4): 411–421.

12. Choi JS, Kim BS, Kim JY, et al. Decellularized extracellular matrix derived from human adipose tissue as a potential scaffold for allograft tissue engineering. *J Biomed Mater Res A* 2011; 97(3): 292–299.

13. Young DA, Ibrahim DO, Hu D, et al. Injectable hydrogel scaffold from decellularized human lipoaspirate. *Acta Biomater* 2011; 7(3): 1040–1049.

14. Sano H, Orbay H, Terashi H, et al. Acellular adipose matrix as a natural scaffold for tissue engineering. *J Plast Reconstr Aesthet Surg* 2014; 67(1): 99–106.

15. Yu C, Bianco J, Brown C, et al. Porous decellularized adipose tissue foams for soft tissue regeneration. *Biomaterials* 2013; 34(13): 3290–3302.

16. Choi JS, Yang HJ, Kim BS, et al. Fabrication of porous extracellular matrix scaffolds from human adipose tissue. *Tissue Eng Part C Methods* 2010; 16(3): 387–396.

17. Pati F, Ha DH, Jang J, et al. Biomimetic 3D tissue printing for soft tissue regeneration. *Biomaterials* 2015; 62: 164–175.

18. Banyard DA, Borad V, Amezcua E, et al. Preparation, characterization, and clinical implications of human decellularized adipose tissue extracellular matrix (hDAM): a comprehensive review. *Aesthet Surg J* 2016; 36(3): 349–357.

19. Song M, Liu Y and Hui L. Preparation and characterization of acellular adipose tissue matrix using a combination of physical and chemical treatments. *Mol Med Rep* 2018; 17(1): 138–146.

20. Dong J, Yu M, Zhang Y, et al. Recent developments and clinical potential on decellularized adipose tissue. *J Biomed Mater Res A* 2018; 106(9): 2563–2574.

21. Kokai LE, Schilling BK, Chnari E, et al. Injectable allograft adipose matrix supports adipogenic tissue remodeling in the nude mouse and human. *Plast Reconstr Surg* 2019; 2: 299e–309e.

22. De Ugarte DA, Ashjian PH, Elbarbary A, et al. Future of fat as raw material for tissue regeneration. *Ann Plast Surg* 2003; 50(2): 215–219.

23. Groenen MA, Archibald AL, Uenishi H, et al. Analyses of pig genomes provide insight into porcine demography and evolution. *Nature* 2012; 491(7424): 393–398.

24. Hussey GS, Dziki JL and Badylak SF. Extracellular matrix-based materials for regenerative medicine. *Nat Rev Mater* 2018; 3: 159–173.

25. Huleihel L, Dziki JL, Bartolacci JG, et al. Macrophage phenotype in response to ECM bioscaffolds. *Semin Immunol* 2017; 29: 2–13.

26. Sicari BM, Dziki JL, Siu BF, et al. The promotion of a constructive macrophage phenotype by solubilized extracellular matrix. *Biomaterials* 2014; 35(30): 8605–8612.

27. Swinehart IT and Badylak SF. Extracellular matrix bioscaffolds in tissue remodeling and morphogenesis. *Dev Dyn* 2016; 245(3): 351–360.

28. Reing JE, Zhang L, Myers-Irvin J, et al. Degradation products of extracellular matrix affect cell migration and proliferation. *Tissue Eng Part A* 2009; 15(3): 605–614.

29. Agrawal V, Tottey S, Johnson SA, et al. Recruitment of progenitor cells by an extracellular matrix cryptic peptide in a mouse model of digit amputation. *Tissue Eng Part A* 2011; 17(19–20): 2435–2443.

30. Huleihel L, Bartolacci JG, Dziki JL, et al. Matrix-bound nanovesicles recapitulate extracellular matrix effects on macrophage phenotype. *Tissue Eng Part A* 2017; 23(21–22): 1283–1294.

31. Dziki JL, Wang DS, Pineda C, et al. Solubilized extracellular matrix bioscaffolds derived from diverse source tissues differentially influence macrophage phenotype. *J Biomed Mater Res A* 2017; 105(1): 138–147.

32. Omidi E, Fuetterer L, Reza Mousavi S, et al. Characterization and assessment of hyperelastic and elastic properties of decellularized human adipose tissues. *J Biomech* 2014; 47(15): 3657–3663.

33. Haddad SM, Omidi E, Flynn LE, et al. Comparative biomechanical study of using decellularized human adipose tissues for post-mastectomy and post-lumpectomy breast reconstruction. *J Mech Behav Biomed Mater* 2016; 57: 235–245.

34. Costa A, Naranjo JD, Turner NJ, et al. Mechanical strength vs. degradation of a biologically-derived surgical mesh over time in a rodent full thickness abdominal wall defect. *Biomaterials* 2016; 108: 81–90.

35. Edwards JH, Ingham E and Herbert A. Decellularisation affects the strain rate dependent and dynamic mechanical properties of a xenogeneic tendon intended for anterior cruciate ligament replacement. *J Mech Behav Biomed Mater* 2019; 91: 18–23.

36. Choi YC, Choi JS, Kim BS, et al. Decellularized extracellular matrix derived from porcine adipose tissue as a xenogeneic biomaterial for tissue engineering. *Tissue Eng Part C Methods* 2012; 18(11): 866–876.

37. Coleman SR and Katzel EB. Fat grafting for facial filling and regeneration. *Clin Plast Surg* 2015; 42(3): 289–300, vii.

38. Kochhar A, Wu I, Mohan R, et al. A comparison of the rheologic properties of an adipose-derived extracellular matrix biomaterial, lipoaspirate, calcium hydroxylapatite, and cross-linked hyaluronic acid. *JAMA Facial Plast Surg* 2014; 16(6): 405–409.

39. Bella J and Hulmes DJ. Fibrillar collagens. *Subcell Biochem* 2017; 82: 457–490.

40. Philp D, Chen SS, Fitzgerald W, et al. Complex extracellular matrices promote tissue-specific stem cell differentiation. *Stem Cells* 2005; 23(2): 288–296.

41. Everitt EA, Malik AB and Hendey B. Fibronectin enhances the migration rate of human neutrophils in vitro. *J Leukoc Biol* 1996; 60(2): 199–206.

42. Kanninen LK, Harjumaki R, Peltoniemi P, et al. Laminin-511 and Laminin-521-based matrices for efficient hepatic specification of human pluripotent stem cells. *Biomaterials* 2016; 103: 86–100.

43. Bonnans C, Chou J and Werb Z. Remodelling the extracellular matrix in development and disease. *Nat Rev Mol Cell Biol* 2014; 12: 786–801.

44. Mariman EC and Wang P. Adipocyte extracellular matrix composition, dynamics and role in obesity. *Cell Mol Life Sci* 2010; 67(8): 1277–1292.

45. Chun TH. Peri-adipocyte ECM remodeling in obesity and adipose tissue fibrosis. *Adipocyte* 2012; 1(2): 89–95.

46. Frith JE, Mills RJ, Hudson JE, et al. Tailored integrin-extracellular matrix interactions to direct human mesenchymal stem cell differentiation. *Stem Cells Dev* 2012; 21(13): 2442–2456.

47. Vaicik MK, Thyboll Kortesmaa J, Moverare-Skrtic S, et al. Laminin alpha4 deficient mice exhibit decreased capacity for adipose tissue expansion and weight gain. *PLoS ONE* 2014; 9(10): e109854.

48. Nie J and Sage EH. SPARC inhibits adipogenesis by its enhancement of beta-catenin signaling. *J Biol Chem* 2009; 284(2): 1279–1290.

49. Simon-Assmann P, Orend G, Mammadova-Bach E, et al. Role of laminins in physiological and pathological angiogenesis. *Int J Dev Biol* 2011; 55(4–5): 455–465.

50. Ingber DE. Extracellular matrix as a solid-state regulator in angiogenesis: identification of new targets for anti-cancer therapy. *Semin Cancer Biol* 1992; 3(2): 57–63.

51. Perumal S, Antipova O and Orgel JP. Collagen fibril architecture, domain organization, and triple-helical conformation govern its proteolysis. *Proc Natl Acad Sci USA* 2008; 105(8): 2824–2829.

52. Vogel V and Sheetz M. Local force and geometry sensing regulate cell functions. *Nat Rev Mol Cell Biol* 2006; 7(4): 265–275.

53. Teong B, Wu SC, Chang CM, et al. The stiffness of a crosslinked hyaluronan hydrogel affects its chondroinduction activity on hADSCs. *J Biomed Mater Res B Appl Biomater* 2018; 106(2): 808–816.

54. Discher DE, Mooney DJ and Zandstra PW. Growth factors, matrices, and forces combine and control stem cells. *Science* 2009; 324(5935): 1673–1677.

55. Yim EK, Pang SW and Leong KW. Synthetic nanostructures inducing differentiation of human mesenchymal stem cells into neuronal lineage. *Exp Cell Res* 2007; 313(9): 1820–1829.

56. Engler AJ, Sen S, Sweeney HL, et al. Matrix elasticity directs stem cell lineage specification. *Cell* 2006; 126(4): 677–689.

57. Dalby MJ, McCloy D, Robertson M, et al. Osteoprogenitor response to semi-ordered and random nanotopographies. *Biomaterials* 2006; 27(15): 2980–2987.

58. Silva GA, Czeisler C, Niece KL, et al. Selective differentiation of neural progenitor cells by high-epitope density nanofibers. *Science* 2004; 303(5662): 1352–1355.

59. Curtis AS and Wilkinson CD. Reactions of cells to topography. *J Biomater Sci Polym Ed* 1998; 12: 1313–1329.

60. Chiquet M, Gelman L, Lutz R, et al. From mechanotransduction to extracellular matrix gene expression in fibroblasts. *Biochim Biophys Acta* 2009; 1793(5): 911–920.

61. Peyton SR and Putnam AJ. Extracellular matrix rigidity governs smooth muscle cell motility in a biphasic fashion. *J Cell Physiol* 2005; 204(1): 198–209.

62. Keane TJ, Swinehart IT and Badylak SF. Methods of tissue decellularization used for preparation of biologic scaffolds and in vivo relevance. *Methods* 2015; 84: 25–34.

63. Tudorache I, Calistru A, Baraki H, et al. Orthotopic replacement of aortic heart valves with tissue-engineered grafts. *Tissue Eng Part A* 2013; 19(15–16): 1686–1694.

64. Wong ML and Griffiths LG. Immunogenicity in xenogeneic scaffold generation: antigen removal vs. decellularization. *Acta Biomater* 2014; 5: 1806–1816.

65. Young DA, Choi YS, Engler AJ, et al. Stimulation of adipogenesis of adult adipose-derived stem cells using substrates that mimic the stiffness of adipose tissue. *Biomaterials* 2013; 34(34): 8581–8588.

66. Kanchwala SK, Holloway L and Bucky LP. Reliable soft tissue augmentation: a clinical comparison of injectable soft-tissue fillers for facial-volume augmentation. *Ann Plast Surg* 2005; 55(1): 30–35; discussion 35.

67. Lemperle G, Morhenn V and Charrier U. Human histology and persistence of various injectable filler substances for soft tissue augmentation. *Aesthetic Plast Surg* 2003; 27(5): 354–366; discussion 367.

68. Turner AE, Yu C, Bianco J, et al. The performance of decellularized adipose tissue microcarriers as an inductive substrate for human adipose-derived stem cells. *Biomaterials* 2012; 33(18): 4490–4499.

69. Pati F, Jang J, Ha DH, et al. Printing three-dimensional tissue analogues with decellularized extracellular matrix bioink. *Nat Commun* 2014; 5: 3935.

70. Kim EJ, Choi JS, Kim JS, et al. Injectable and thermosensitive soluble extracellular matrix and methylcellulose hydrogels for stem cell delivery in skin wounds. *Biomacromolecules* 2016; 17(1): 4–11.

71. Cheung HK, Han TTY, Marecak DM, et al. Composite hydrogel scaffolds incorporating decellularized adipose tissue for soft tissue engineering with adipose-derived stem cells. *Biomaterials* 2014; 35(6): 1914–1923.

72. Kayabolen A, Keskin D, Aykan A, et al. Native extracellular matrix/fibroin hydrogels for adipose tissue engineering with enhanced vascularization. *Biomed Mater* 2017; 12(3): 035007.

73. Zielins ER, Brett EA, Longaker MT, et al. Autologous fat grafting: the science behind the surgery. *Aesthet Surg J* 2016; 36(4): 488–496.

74. Khouri RK Jr and Khouri RK. Current clinical applications of fat grafting. *Plast Reconstr Surg* 2017; 140(3): 466e–486e.

75. LoTempio MM and Allen RJ. Breast reconstruction with SGAP and IGAP flaps. *Plast Reconstr Surg* 2010; 126(2): 393–401.

76. Rubin JP and Smith D. Discussion: percutaneous aponeurotomy and lipofilling: a regenerative alternative to flap reconstruction? *Plast Reconstr Surg* 2013; 5: 1291–1292.

77. Debels H, Gerrand YW, Poon CJ, et al. An adipogenic gel for surgical reconstruction of the subcutaneous fat layer in a rat model. *J Tissue Eng Regen Med* 2017; 11(4): 1230–1241.

78. Orbay H, Takami Y, Hyakusoku H, et al. Acellular dermal matrix seeded with adipose-derived stem cells as a subcutaneous implant. *Aesthetic Plast Surg* 2011; 35(5): 756–763.

79. Gentleman E, Nauman EA, Livesay GA, et al. Collagen composite biomaterials resist contraction while allowing development of adipocytic soft tissue in vitro. *Tissue Eng* 2006; 12(6): 1639–1649.

80. Adam Young D, Bajaj V and Christman KL. Award winner for outstanding research in the PhD category, 2014 society for biomaterials annual meeting and exposition, Denver, Colorado, 16–19 April, 2014: decellularized adipose matrix hydrogels stimulate in vivo neovascularization and adipose formation. *J Biomed Mater Res A* 2014; 102(6): 1641–1651.

81. Wang L, Johnson JA, Zhang Q, et al. Combining decellularized human adipose tissue extracellular matrix and adipose-derived stem cells for adipose tissue engineering. *Acta Biomater* 2013; 9(11): 8921–8931.

82. Poon CJ, Pereira E, Cotta MV, Sinha S, et al. Preparation of an adipogenic hydrogel from subcutaneous adipose tissue. *Acta Biomater* 2013; 9(3): 5609–5620.

83. Han TT, Toutounji S, Amsden BG, et al. Adipose-derived stromal cells mediate in vivo adipogenesis, angiogenesis and inflammation in decellularized adipose tissue bioscaffolds. *Biomaterials* 2015; 72: 125–137.

84. Lu Q, Li M, Zou Y, et al. Delivery of basic fibroblast growth factors from heparinized decellularized adipose tissue stimulates potent de novo adipogenesis. *J Control Release* 2014; 174: 43–50.

85. Zhang S, Lu Q, Cao T, et al. Adipose tissue and extracellular matrix development by injectable decellularized adipose matrix loaded with basic fibroblast growth factor. *Plast Reconstr Surg* 2016; 137(4): 1171–1180.

86. Cho SW, Kim I, Kim SH, et al. Enhancement of adipose tissue formation by implantation of adipogenic-differentiated preadipocytes. *Biochem Biophys Res Commun* 2006; 345(2): 588–594.

87. Torio-Padron N, Baerlecken N, Momeni A, et al. Engineering of adipose tissue by injection of human preadipocytes in fibrin. *Aesthetic Plast Surg* 2007; 31(3): 285–293.

88. Roehm KD, Hornberger J and Madihally SV. In vitro characterization of acellular porcine adipose tissue matrix for use as a tissue regenerative scaffold. *J Biomed Mater Res A* 2016; 104(12): 3127–3136.

89. Wang JK, Luo B, Guneta V, et al. Supercritical carbon dioxide extracted extracellular matrix material from adipose tissue. *Mater Sci Eng C Mater Biol Appl* 2017; 75: 349–358.

90. Crapo PM, Gilbert TW and Badylak SF. An overview of tissue and whole organ decellularization processes. *Biomaterials* 2011; 32(12): 3233–3243.

91. Goh SK, Bertera S, Olsen P, et al. Perfusion-decellularized pancreas as a natural 3D scaffold for pancreatic tissue and whole organ engineering. *Biomaterials* 2013; 34(28): 6760–6772.

92. Buhler NE, Schulze-Osthoff K, Konigsrainer A, et al. Controlled processing of a full-sized porcine liver to a decellularized matrix in 24 H. *J Biosci Bioeng* 2015; 119(5): 609–613.